Mechanism of excitation of nonlinear capillary waves on the surface of a liquid metal in contact with a dense plasma

M. D. Gabovich and V. Ya. Poritskiĭ

Physics Institute, Ukrainian Academy of Sciences
(Submitted 14 December 1982)
Zh. Eksp. Teor. Fiz. **85**, 146–154 (July 1983)

Panoramas are obtained of nonlinear capillary waves excited on the surface of a liquid metal in contact with a dense unstable plasma, and also on the rear side of a liquid-metal layer whose front side is in contact with the indicated plasma. It is shown that on the rear side of the liquid-metal layer the excitation of the waves and their form are due to parametric instability caused by vibration of the metal under the influence of a strong ion flux modulated by the plasma oscillations. On the liquid-metal surface in contact with an unstable plasma, the form of the observed peaks is determined by the action of a strong electric field localized on the crests of the waves excited by the generated ultrasound.

PACS numbers: 68.10.Gw

INTRODUCTION

A panoramic picture of nonlinear capillary waves generated on the surface of a liquid metal in contact with a dense plasma was first recorded in Ref. 1. Long ago Tonks and Frenkel[2,3] pointed out a possible mechanism for the onset of an aperiodic instability $(\omega^2 < 0)$ of this surface when acted upon by a sufficiently strong electric field—the initial perturbation of the surface causes a local-field increase that determines the further growth of the perturbation, etc. The critical field is determined directly from the corresponding dispersion equation[4]

$$\omega^2 = \frac{k}{\rho}\left(\sigma k^2 + \rho g - \frac{E^2}{4\pi}k\right), \tag{1}$$

where g is the free-fall acceleration, σ is the surface tension, ρ is the density, and $k = 2\pi/\lambda$ is the wave number. If we confine ourselves the short capillary waves $(\sigma k^2 \gg \rho g)$ considered below the critical field is

$$E_{cr} = [4\pi\sigma k]^{1/2}. \tag{2}$$

Interest in the study of nonlinear capillary waves excited as a result of the Tonks-Frenkel' instability is due both to a number of important applied problems, e.g., the development of liquid-metal ion sources, which emit in a field $E \approx 10^8$ V/cm an ion flux of density $j_+ \approx 10^5$ A/cm²,[5] as well as to the discovery of instability of a charged liquid-helium surface in an electric field[6] and of the surface of a ferromagnetic liquid in a magnetic field.[7]

The present study differs from the preceding experimental investigations in that the electric field is produced not by an external electrode,[8] but by a space charge of ions in the region of the contact of the liquid metal with a dense plasma (in the Debye layer). Another novelty is the use of the method of "freezing" the wave surface followed by an investigation of its radiation by a high-resolution raster electron microscope.

The main purpose of the study is the determination of the physical processes that effect the connection between a dense unstable plasma and capillary waves on a liquid-metal surface in contact with the plasma.

PROCEDURE, RESULTS AND THEIR DISCUSSION

The surface of an electrode having a negative potential U relative to the plasma is acted upon by an electric field

$$E = (16\pi j_+)^{1/2}(2e/M)^{-1/4}U^{1/4}, \tag{3}$$

where e and M are the charge and mass of the ions, j_+ is the density of the ion current from the plasma boundary into a positive space-charge layer of width

$$d_l = (1/9\pi)^{1/2}(2e/M)^{1/4}U^{3/4}j_+^{-1/2}. \tag{4}$$

At sufficiently large j_+ and U the field E can reach the critical value determined by Eq. (2). Such conditions were produced by a unit that produced in vacuum a plasma column of radius ~ 1 mm, propagating in a magnetic field $H = 10$ kOe and making it possible to obtain on the target a flux of ions of different gases with a current density up to 100 A/cm² in a continuous regime (Fig. 1). It was possible to apply to the target, without striking an arc, a negative potential up to 500 V relative to the plasma, so that the specific power of the ion flux reached $w \approx 0.5 \times 10^5$ W/cm²; of course in this case the ion flux contained, besides the gas ions ionized in the plasma (in the region of the plasma flare) also sputtered and evaporated atoms of the target metal. At the indicated specific power the metal penetrates to a depth h and the momentum is transferred to the liquid metal and ejects it to the "cold edge"—to the periphery of the crater (Fig. 2). After the plasma source is turned off and the metal hardens, the waves produced on its surface are fixed; the surface waves fixed in this manner were investigated with an electron microscope having a resolution ≈ 100 Å.
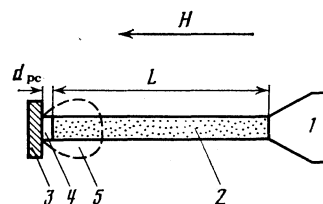

FIG. 1. Experimental setup: 1—plasma source, 2—plasma column, 3—target, 4—positive space-charge layer, 5—plasma flare.
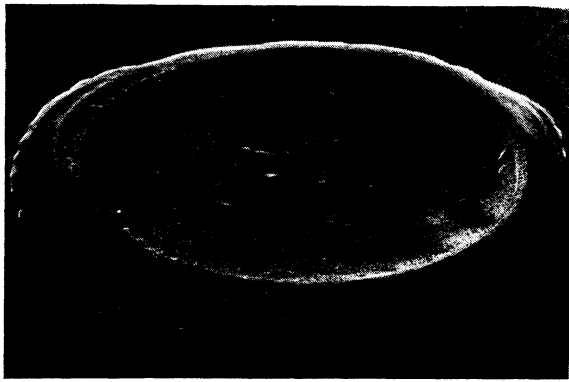
FIG. 2. Crater produced by ion stream.

Figure 3a shows the panorama obtained in this manner of the nonlinear waves produced on the surface of a thick copper sample. Individual fragements of the panorama show the detail of the peaks, particularly the peak on the vertex of which the metal drop is "frozen" at the instant of detachment. (A similar detachment of drops is known and was established by many workers observing the integral flux of these drops under the action of an electric field on the liquid metal.) The peaks are disposed as a rule along radial crests spaced 500–70 μm apart. The average distance between peaks is 10–20 μm.

It is necessary to consider first the fixation of the "freezing" capillary waves. It is known[10] that the damping coefficient of the latter is $\gamma = 2\eta k^2/\rho$, where η is the viscosity, while the relaxation time for the heat-conduction process is $\tau \sim l^2 \rho c/x$, where l is the characteristic dimension of the
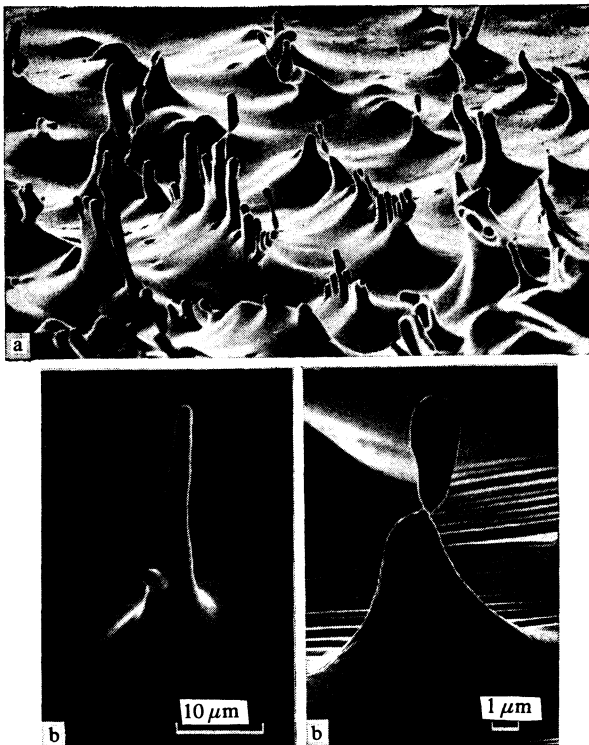
freezing region, x is the thermal conductivity coefficient, and c is the specific heat. The waves are fixed at $1/\gamma \gg \tau$, and consequently the sought condition can be represented in the form

$$x \gg 2l^2 k^2 \eta c. \tag{5}$$

At a large depth of the melt (in our case, directly below the stream), when $l^2 k^2 = h^2 k^2 \gg 1$, no fixing takes place, the waves are damped before the solidification of the metal, but outside the main stream, at $l = \lambda$, the relation (5) is satisfied, for example, for iron and copper. For titanium, however, the inverse inequality holds. In accord with these estimates, the freezing of the surface waves is observed on copper and stainless steel, but not on titanium. The small sizes of the peaks determined also the rapid dissipation of the released heat of crystallization. A clear demonstration of the latter is the freezing of the drops at the instant of their detachment (Fig. 3c).

The threshold character of the excitation of nonlinear capillary waves follow from the fact that the excitation of these waves ceases when the specific power is decreased by only several times. Figure 4 was obtained under conditions close to the limiting ones, when there are no peaks but smoothed radial wave crests still remain. Even though it was possible to fix a panorama similar to that of Fig. 4 on pure metal, to fix waves with smoothed crests more distinctly it was necessary to resort to an artifice. Namely, the target was bombarded simultaneously with nitrogen and titanium ions. A very thin but easily identifiable layer of refractory titanium nitride appeared on the surface. The earlier solidification of this layer contributed to the fixing of the radial crests of the waves. We note incidentally that here, just as in other cases, one cannot exclude the melt rotation due to interaction of the radial component of the current in the metal with the external magnetic field.

As for the shape of the observed nonlinear waves (Fig.

FIG. 3. Panorama of frozen waves fixed on the surface of a bulky copper target (a) and fragments of the panorama.
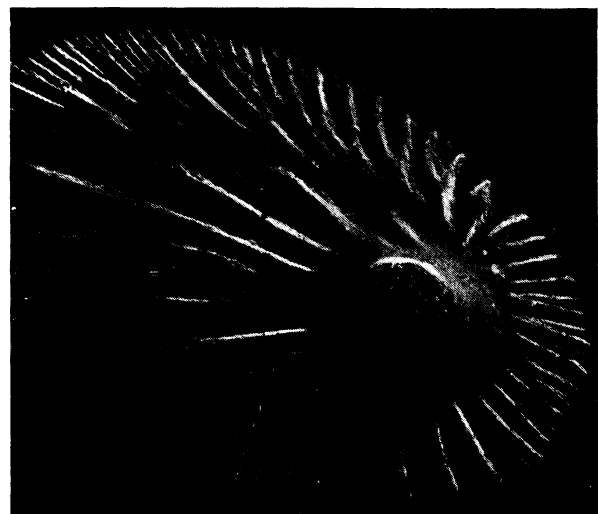

FIG. 4. Panorama of fixed waves obtained on the surface of stainless steel when the stream strength is decreased.

3), it contradicts neither the Tonks model calculations[2] nor the computer numerical results.[11] The first stage concludes with formation of a hemispherical or conical projection. During the second stage no additional liquid flows in, but the vertex of the cone lengthens, and a peak with decreased curvature radius is produced on it. Yet a disparity between the critical field calculated from Eq. (2) and its actual value needed to observe the instability, on the one hand, and those calculated from Eq. (3) following substitution in it of the measured values of j_+ and U, was noted back in Ref. 1. Whereas substitution in (2) of the measured wavelengths yields $E_{cr} \approx 10^6$ V/cm, the field calculated from (3) is $\approx 10^5$ V/cm (for the measured values $j_+ = 100$ A/cm^2, $U = 500$ V, and $M = 1.6 \times 10^{-24}$ g). Such a difference makes difficult a natural explanation of the observed effects as being due to the Tonks-Frenkel' instability and prompts us to pay attention to the possible role of the oscillations in the plasma column. A direct analysis of the ion flux incident on the target points to the existence of a whole spectrum of oscillations that seem to differ in character. Against the background of relatively weak oscillations, however, there appears distinctly the peak shown in Fig. 5. The frequency corresponding to this peak change with change of the plasma-current discharge on the current I_p approximately in proportion to $I_p^{1/2}$, depends little on the magnetic field intensity, and decreases noticeably with increasing mass of the ions. At large discharge currents the growth of the frequency with increasing current slow down and under these conditions the frequency is 1.3 and 0.4 MHz for hydrogen and nitrogen plasma, respectively.

The ionic vibrations in the plasma are described by the known dispersion relation

$$\omega_0 = \omega_+ \left(1 + \frac{1}{k_1^2 d_e^2}\right)^{-1/2}, \tag{6}$$

where $\omega_+ = (4\pi n_+ e/M)^{1/2}$ is the frequency of the ion Langmuir oscillations; $k_1 = 2\pi/\lambda_1$ is the wave number and can be
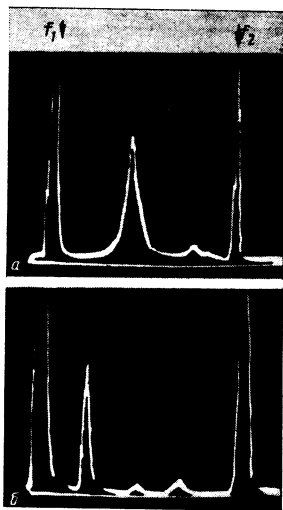

FIG. 5. Frequency spectra of the current oscillations in the target circuit: a) hydrogen: $I_p = 4$ A, $H = 10$ kOe; frequency markers $f_1 = 0, f_2 = 2.5$ MHz; b) nitrogen: $I_p = 7$ A, $H = 10$ kOe; frequency markers $f_1 = 0$, $f_2 = 2.4$ MHz.

estimated by specifying a wavelength equal to double the length L of the plasma column,[12] and $d_e = (T_e/4\pi n_e e^2)^{1/2}$ is the Debye length.

Under the experimental conditions, on the axis of a plasma column of length $L = 5$ cm at an ion-current density $j_+ \sim 100$ A/cm^2, the charged-particle density is $n_+ \approx n_e \approx 5 \times 10^{14}$ cm^{-3} and $T_e \approx 10$ eV, and consequently $d_e \approx 10^{-4}$ cm. Since $k_1 d_e \ll 1$ it follows from (6) that an ion-acoustic mode should be excited with a frequency.

$$f_0 = \frac{\omega_0}{2\pi} = \frac{2}{L}\left(\frac{T_e}{M}\right)^{1/2} \approx 10^6 \text{ Hz}$$

(for hydrogen), as is in fact observed.

Excitation of ion-acoustic oscillations under conditions close to the foregoing was investigated by Nezlin.[12] If account is taken of the measured degree of modulation of the total ion current, 15%, as well as of the corresponding modulation of the plasma potential, the modulation of the average specific power is approximately 30%; the modulation of the local specific power is substantially larger, as established directly by probe measurements.

It is known that for an unperturbed liquid surface the kinetic pressure exerted on all the ions accelerated in the layer at an accommodation coefficient equal to unit are completely cancelled out by the negative electrostatic pressure $E^2/8\pi$, and the pressure connected with the electrons reflected in the layer by the electrons is relatively small. The principal role is played by the pressure produced by the recoil of the neutral atoms that leave the surface as a result of cathode sputtering an evaporation; this pressure equals

$$p = \alpha w v_a/Q, \tag{7}$$

where v_a is the average velocity of the emitted neutral particles, Q is the energy needed to remove a unit mass, and $\alpha \approx 1$. With the aid of (3) and (7) it can be verified that under the experimental conditions, independently of the value of j^+, the pressure $p \gg E^2 8\pi$. It follows from (7) that modulation of w at the frequency of the plasma oscillations can lead to generation of ultrasound (see also Ref. 14). For an experimental confirmation of the latter, the target thickness was decreased to a value ($h \approx 3$ mm) such that the target was melted through its entire depth in the region of incidence of the ion stream. Fragments of the panoramas obtained simultaneously on the front and rear sides of the target are shown in Figs. 6a and 6b. It turns out that on the rear side, where there is no plasma or electric field whatever, a perfectly distinct picture of frozen surface wave was fixed, and it is natural to attribute its appearance to ultrasound generation. The picture observed on Fig. 6b cannot be directly attributed to displacement of the surface under the action of the pressure p modulated at a frequency ω_0. Such a displacement $\xi_0 = p/\rho c_s \omega_0$ (where c_s is the speed of sound) would not exceed under the conditions of the described experiment 100 Å. Under certain conditions, however, the amplitude of standing capillary waves on a liquid surface subjected to vibrations increases expoentially.[15] Such an increase calls for satisfaction of two conditions. The amplitude ξ_0 of the initial displacement must exceed a certain critical value $\xi_{cr} = 4\eta k/\rho\omega_0$, and the frequency of the capillary waves must satisfy the
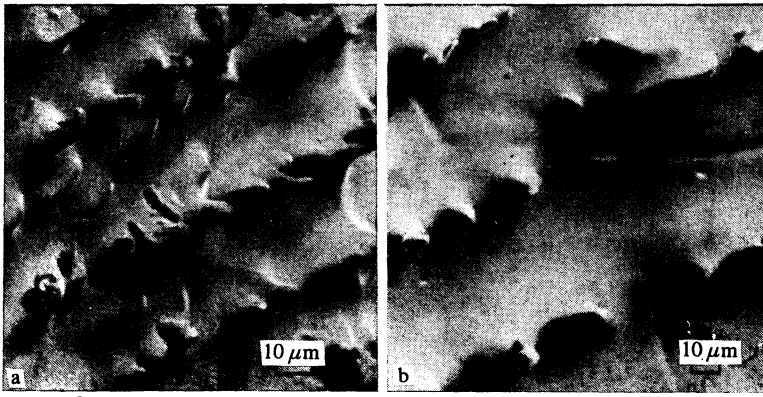
                    M. D. Gabovich and V. Ya. Poritskiĭ   88

FIG. 6. Panoramas of frozen waves: a—on the front side of a copper target; b—on the rear side; c—fragement of panorama on the rear side.

equality $\omega = (\sigma k^3/\rho)^{1/2} = \omega_0/2$. The first condition, taking (7) into account, reduces to

$$w \geqslant 4\eta kc_s Q/v_a. \qquad (8)$$

Putting $\eta = 10^{-2}$ P, $Q = 5 \times 10^{10}$ erg/g, $\lambda = 5 \times 10^{-3}$ cm, and $c_s < v_a < 10c_s$ (v_a can greatly exceed the speed of sound because of the predominant role of current sputtering), we obtain $w \geqslant 10^4$ W/cm^2, which agrees in order of magnitude with the experimental data; if we assume a Gaussian distribution of the density in the plasma column, the specific power on the axis, calculated from the measured flux power and from the maximum power received by the probe crossing the axis, is equal to $w_0 = 0.4 \times 10^5$ W/cm^2 in the case shown in Fig. 3. From the second condition we obtain independently $\lambda \approx 10^{-3}$ cm, which is likewise not outside the range of the observed wavelengths. Of course, for various reasons the accuracy of the estimates presented must not be overestimated. We note, in particular that in the calculation of Ref. 15 a quadratic lattice of standing waves ($\xi = 1/2q(t)(\cos kx + \cos ky)$) was considered, but under our conditions the lattice lines are radial or circular. Moreover, as shown by Fig. 7 on the periphery, the radial crests of the waves and the peaks on them, concentrated in the form of isolated braids, form closed loops. The number of braids can range from a few units to several dozen. Thus, the obtained surface-wave panoramas (Fig. 6b) and the satisfactory agreement between the results of independent estimates of the specific threshold power and the wavelength, on the one hand, and the experimental data, on the other, lead to the conclusion that what was fixed on the rear side was parametric instability of the capillary waves, due to vibration of the liquid-metal surface under the action of the ion stream modulated by the plasma oscillations. Similar peaks, appear, naturally, also on the front side, where in fact the ultrasound is excited. The front side, however, unlike the rear, is subjected also to the action of the electric field and of ion bombardment. Unfortunately, a theoretical analysis of the instability of the surface of the liquid metal when simultaneoulsy acted by ultrasound and alternating and constant electric fields, and also by the ion stream, has not yet been performed. Nonetheless, since the negative pressure that increases the perturbation on the liquid-metal surface on account of the action of the electric field ($E^2/8\pi$) depends substantially on the curvature radius of the perturbation, it follows that the electric-field action produced on top of the ultrasound can be identified by the
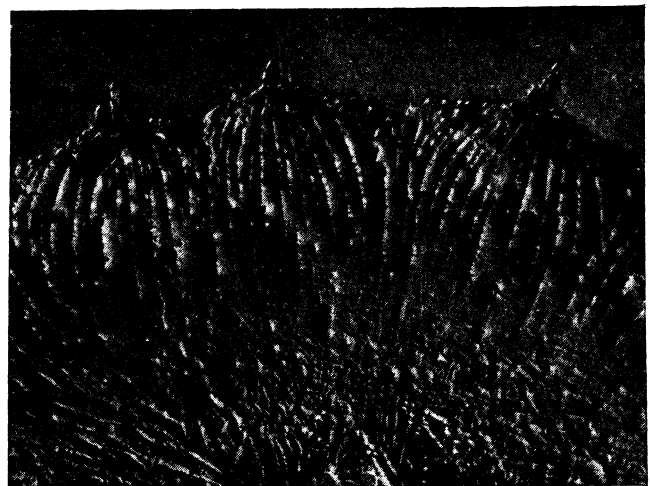

FIG. 7. Fragment of panorama of frozen wave on the rear side of a stainless-steel target. Central part—melt-through region, where the waves are not fixed.

appearance of peaks with decreasing curvature radii. The corresponding difference between the shapes of the peaks can in fact be established by comparing Figs. 3 and 6c, obtained under extreme conditions: at maximum electric field and in its absence. The facts presented offer evidence that the panorama of Fig. 3 is the result of joint action of ultrasound and an electric field. In this case the role of the ultrasound manifests itself in formation of nonlinear waves on the crests of which is realized an electric field Er such that $E_r^2/8\pi > 2\sigma/r$, where r is the curvature radius of the peaks.

Of fundamental significance is also the established identity of the panoramas obtained on the rear side of the target when it is melted through by the ion stream drawn from an unstable plasma, as well as by a strong electric beam not subjected to external modulation; in both cases the panorama takes the form shown in Fig. 7. A detailed study of this phenomenon is a separate problem. It is important to point out only the fact that in a powerful welding electron beam there are excited ionic oscillations[16] with frequencies close to the indicated ion-sound oscillations of the plasma column. Thus, a powerful electron beam turns out to be density-modulated and is capable of generation ultrasound and of exciting nonlinear capillary waves by the mechanism considered above.

CONCLUSION

We have shown in this paper that when a dense unstable plasma comes in contact with a liquid metal nonlineary capillary waves are produced under the influence of the ultrasound excited by an ion beam having a high specific power and modulated by the plasma oscillations. The structure of the obtained panoramas of the nonlinear capillary waves (the wavelength) is determined by the ultrasound, since the recoil pressure of the neutral atoms sputtered by the ions from the surface of the liquid metal exceeds considerably the maximum value of the negative electrostatic pressure $E^2/8\pi$ for an unperturbed surface. The shape of the peaks, however, depends on the presence of an electric field near the surface.

Joint action of ultrasound and of a sufficiently strong electric field can cause the peaks to assume the form typical of the Tonks-Frenkel' instability seen in the case when the field determined by (2) is lower than critical.

Nonlinear capillary waves can be realized also when the metal interacts with high-power electron beams that are modulated in density as they propagate under ordinary vacuum conditions and also cause generation of ultrasound.

[1]M. D. Gabovich and V. Ya. Poritskii, Pis'ma Zh. Eksp. Teor. Fiz. **33**, 320 (1981) [JETP Lett. **33**, 304 (1981)].

[2]L. Tonks, Phys. Rev. **48**, 562 (1935).

[3]Ya. I. Frenkel', Phys. Zs. Sowjetunion **8**, 675 (1935).

[4]L. D. Landau and E. M. Lifshitz, Electrodynamcis of Continuous Media, Pergamon, 1969.

[5]R. Clampitt, K. L. Aitken, and D. K. Jefferies, J. Vac. Sci. Technol. **12**, 1208 (1975).

[6]L. P. Gor'kov and D. M. Chernikova, Dokl. Akad. Nauk SSSR 228, 829 (1976) [Sov. Phys. Doklady **21**, 328 (1976)].

[7]M. N. Shliomis, Usp. Fiz. Nauk **112**, 427 (1974) [Sov. Phys. Usp. **17**, 153 (1974)].

[8]P. Yu. Bartashyus, L. I.Panevichyus, and G. N. Fursei, Zh. Tekh. Fiz. **41**, 1943 (1971) [Sov. Phys. Tech. Phys. **16**, 1535 (1972)].

[9]B. E. Paton, M. D. Gabovich, et al., Dokl.Akad. Nauk **239**, 576 (1978) [Sov. Phys. Dokl. **23**, 205 (1978)].

[10]L. D. Landau and E. M. Lifshitz, Fluid Mechanics, Pergamon, 1959.

[11]L. M. Baskin, Yu. F. Matyushichev, and G. N. Fursei, Abstracts, All-Union Symp. on Nonincandescent Cathodes, Tomsk, 1980, p. 78.

[12]M. V. Nezlin, Dinamika puchkov v plazme [Dynamics of Beams in a Plasma], Energoizdat, 1982, p. 135.

[13]L. Tonks, Phys. Rev. **46**, 278 (1934).

[14]G. A. Askar'yan and E. M. Moroz, Zh. Eksp. Teor. Fiz. **43**, 2319 (1962) [Sov. Phys. JETP **16**, 1638 (1963)].

[15]O. K. Eknadiosyants, Formation of Aerosols, in: Fizicheskie osnovy ul'trazvukovoĭ tekhnologii (Physical Principles of Ultrasound Technology), L. D. Rozenberg, ed., Nauka, 1970, p. 370.

[16]V. P. Kovalenko and S. K. Pats'ora, Zh. Eksp. Teor. Fiz. **77**, 909 (1979) [Sov. Phys. JETP **50**, 458 (1979)].

Translated by J. G. Adashko